Concave Nanoparticles

DOI: 10.1002/ange.201105200

Silver Nanocrystals with Concave Surfaces and Their Optical and Surface-Enhanced Raman Scattering Properties**

*Xiaohu Xia, Jie Zeng, Brenden McDearmon, Yiqun Zheng, Qingge Li, and Younan Xia**

Silver nanocrystals with well-defined and controllable shapes or morphologies have attracted ever increasing attention due to their remarkable optical properties and applications related to surface plasmon resonance (SPR), surface-enhanced Raman scattering (SERS), optical labeling, and biological sensing.[1] Thanks to the efforts from a large number of research groups, a myriad of Ag nanocrystals with different shapes such as spheres, cubes, octahedrons, bars, bipyramids, plates, decahedrons, and rods/wires have been prepared with reasonable quality and quantity.[2] Essentially, all of these Ag nanocrystals are enclosed by a convex surface and low-index facets. Parallel to the convex systems, nanocrystals with concave surfaces have started to receive interests in recent years owning to their distinctive optical and catalytic properties.[3] Although a number of noble metals including Au, Pd, Pt, Rh, and some of their bimetallic combinations have been prepared as nanocrystals with concave surfaces,[3,4] to our knowledge, no concave nanocrystals made of Ag have been reported in literature.

Herein, we describe a facile approach to the synthesis of Ag concave nanocrystals via seed-mediated growth. The synthesis involved the use of Ag nanocubes as seeds in an aqueous system, with L-ascorbic acid (AA) serving as a reductant and $AgNO_3$ as a salt precursor. For this simple system, we found that increasing the concentration of AA accelerated the deposition rate of Ag atoms on the side faces of a cubic seed along the ⟨100⟩ directions, resulting in the formation of an octahedron with a concave structure on each one of its faces. When Cu^{2+} ions were introduced, however, growth was dominated by the ⟨111⟩ directions, forcing the cubic seed to sequentially evolve into a concave cube, an octapod, and finally a concave trisoctahedron, with all of them being enclosed by high-index facets.

In a standard synthesis (see Supporting Information) of Ag concave octahedrons, an aqueous $AgNO_3$ solution was added with a syringe pump into a mixture of AA and Ag seeds under magnetic stirring. The seeds were 40 nm nanocubes with slight truncation at the corners and probably edges (see Figure S1a in the Supporting Information). Figure 1 a,b, shows SEM and TEM images of the product obtained using the standard procedure. The product had a uniform distribution in terms of both shape and size. The SEM image implies that the product still had an octahedral morphology with an average size (defined as the distance between adjacent vertexes, see Figure S2) of 80 nm, with each side face of the octahedron being excavated by a curved cavity in the center. As clearly shown by the TEM images in Figure 1 d (bottom

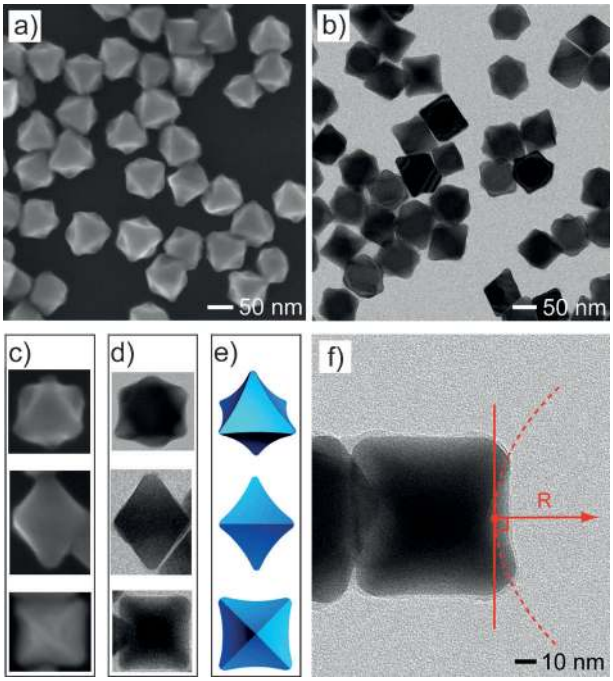

Figure 1. a) SEM and b) TEM images of Ag concave octahedrons prepared from Ag cubic seeds using a standard procedure. c) SEM images, d) TEM images, and e) models of a concave octahedron orientated along ⟨111⟩ (top panel), ⟨110⟩ (middle panel), and ⟨100⟩ (bottom panel) directions, respectively. f) TEM image of a single concave octahedron orientated along <100> direction at a higher magnification. The dash line indicates the concave face with a curvature of *R* in radius.

[*] X. Xia,[+] Dr. J. Zeng,[+] B. McDearmon, Y. Zheng, Prof. Y. Xia
Department of Biomedical Engineering, Washington University
St. Louis, MO 63130 (USA)
E-mail: xia@biomed.wustl.edu
X. Xia,[+] Dr. Q. Li
Engineering Research Center of Molecular Diagnostics
School of Life Sciences, Xiamen University
Xiamen, Fujian 361005 (P.R. China)
[+] These authors contributed equally to this work.

[**] This work was supported by research grants from the NSF (DMR, 0804088 and 1104616) and startup funds from the Washington University in St. Louis. As a jointly supervised Ph.D. student from Xiamen University, X.X. was also supported by a Fellowship from the China Scholarship Council. Part of the research was performed at the Nano Research Facility, a member of the National Nanotechnology Infrastructure Network (NNIN), which is funded by the NSF under award no. ECS-0335765.

Supporting information for this article (detailed experimental protocols for syntheses of various types of Ag nanostructures, as well as their characterizations) is available on the WWW under http://dx.doi.org/10.1002/anie.201105200.

panel), the concave octahedron exhibited a darker contrast for the diagonals as compared to the other areas when viewed along the ⟨100⟩ direction, confirming the formation of a concave structure on the surface. The radius of curvature (R) for the face of such a concave octahedron was estimated to be 130 nm based on the TEM image in Figure 1 f. The additional SEM image in Figure S3a demonstrated that the concave octahedrons could be obtained in high purity (> 95 %) and relatively large quantity.

The standard procedure (see Supporting Information) for synthesizing Ag concave trisoctahedrons was similar to what was used for concave octahedrons except for the introduction of $Cu(NO_3)_2$ into the reaction solution. Figure 2 a,b, shows SEM and TEM images of a product obtained under the new conditions. The SEM image indicates that the particles had a concave, trisoctahedral morphology, which is more or less similar to that of the Au trisoctahedron reported by Xie and co-workers.[5] They had an average size (defined as the distance between adjacent vertexes along the ⟨110⟩ axis, see Figure S2b) of ca. 100 nm and contained eight trigonal pyramids on the surface. Different from the case of Au trisoctahedrons, the corners of Ag trisoctahedrons were found to be significantly truncated. Figure 2 c shows models of the Ag trisoctahedrons in three different orientations corresponding to those labeled in Figure 2 a,b. Figure 2 d shows an individual Ag trisoctahedron viewed along the ⟨110⟩ direction, where 4 of the 24 faces of a trisoctahedron can be projected edge-on (see the model shown in Figure S4a). The Miller indices of the edge-on facets of a trisoctahedron can be determined by analyzing the projection angles.[6] By comparing the measured projection angles (Figure 2 d) with the calculated ones (Figure S4b), these 4 edge-on facets could be indexed as the {221} planes. The Miller indices of a high-index facet can also be determined from the atomic arrangements.[6] Figure 2 e shows high-resolution TEM image of one edge-on facet of the Ag trisoctahedron viewed along the $[1\bar{1}0]$ zone axis, as confirmed by the corresponding Fourier transform (FT) pattern. The atomic arrangement was composed of a series of (111) terrace of three atomic widths with one (110) step, resulting in an overall profile indexed as the (221) planes. This observation is consistent with the atomic model of a (221) plane shown in Figure 2 f. Some of the trisoctahedrons did not perfectly match the model of a trisoctahedron enclosed by {221} facets, and tended to be enclosed by {331} or {332} facets as revealed by the projection angles (see Figure S4c,d). The additional SEM image shown in Figure S3b also demonstrates that the Ag concave trisoctahedrons could be obtained with purity close to 100 %.

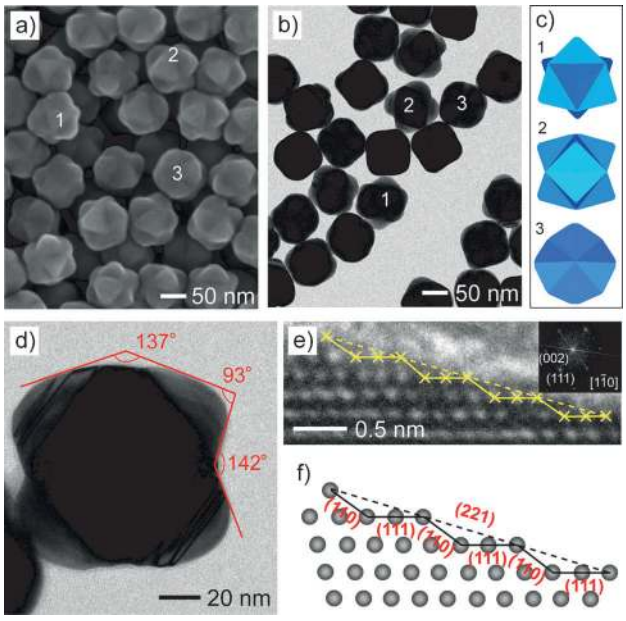

Figure 2. a) SEM and b) TEM images of Ag concave trisoctahedrons prepared from Ag cubic seeds using a standard procedure. c) Models of an ideal concave trisoctahedron orientated along ⟨111⟩ (top), ⟨110⟩ (middle), and ⟨100⟩ (bottom) directions, respectively, corresponding to the nanocrystals marked with the same numbers in (a) and (b). d) TEM image of a single concave octahedron at a higher magnification viewed along ⟨110⟩ direction. e) HRTEM image of an edge-on facet viewed along the ⟨110⟩ direction showing the {221} facets. The centers of surface atoms are indicated by "×". f) The atom model of (221) planes projected from the $[1\bar{1}0]$ zone axis. The (221) planes can be visualized as a combination of a (111) terrace of three atomic widths with one (110) step.

It should be pointed out that the size of the Ag concave nanocrystals could be readily controlled by using cubic seeds with different sizes. For example, Ag concave octahedrons and trisoctahedrons with average sizes of 32 and 45 nm (see Figure S5a,b), respectively, could be obtained by using Ag nanocubes with an average edge length of 23 nm (Figure S1b) as the seeds. In addition, 120 nm concave octahedrons and 150 nm trisoctahedrons (Figure S5c,d) could be obtained by using Ag nanocubes with an average edge length of 60 nm (Figure S1c) as the seeds. SEM images taken from the products indicate that the concave structure was well maintained in the final nanocrystals regardless of particle size.

To gain insight into the details of morphological evolution for the Ag concave octahedrons and trisoctahedrons, aliquots of the reaction solution were taken out after different volumes of the $AgNO_3$ precursor solution had been injected, followed by examinations using SEM and UV-vis spectroscopy. Figure 3 a–d, shows SEM images and models that illustrate the evolution from cubic seeds to concave octahedrons. In the initial stage of the reaction (Figure 3 a, 0.8 mL of $AgNO_3$), the seeds had grown into truncated cubes. This observation suggests that the newly formed Ag atoms were mainly deposited on {100} facets of the seeds. As the amount of $AgNO_3$ solution was increased to 2.0 mL (Figure 3 b), cuboctahedrons with protuberant edges and corners were observed. After 4.0 mL of $AgNO_3$ solution had been added (Figure 3 c), the product had become truncated octahedrons with concave side faces. Due to the increase in size, the concave structure became more obvious under SEM. When the amount of $AgNO_3$ solution was increased to 5.0 mL (Figure 3 d), concave octahedrons of ca. 80 nm in edge length were obtained. These observations suggest that, during the morphological transition from nanocubes to concave truncated cubes, cuboctahedrons, truncated octahedrons, and concave octahedrons, the growth prevailed along the ⟨100⟩ directions. Further increase of the precursor to 7.0 mL (Figure S6a) did not result in further changes to size and

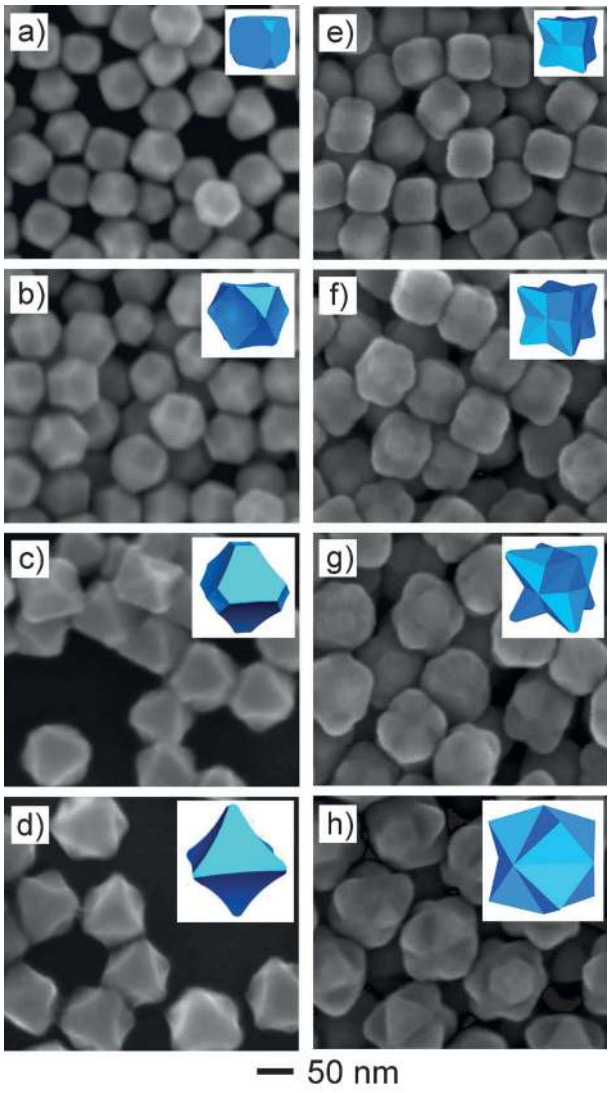

Figure 3. SEM images showing the evolution of: a–d) Ag concave octahedrons in a standard synthesis and e–h) Ag concave trisoctahedrons in a standard synthesis. The volume of $AgNO_3$ injected was a) 0.8, b) 2, c) 4, d) 5, e) 1.5, f) 3.5, g) 6.5, and h) 10 mL, respectively. The insets illustrate the corresponding model for each nanocrystal.

morphology for the concave octahedrons. However, irregular particles started to appear in the product due to homogeneous nucleation and growth. Figure 3e–h, shows SEM images and models corresponding to shape evolution from cubic seeds to concave trisoctahedrons. In the initial stage of the reaction (Figure 3e, 1.5 mL of $AgNO_3$), the seeds had grown into cubes with protuberances at corners, a morphology similar to that of a concave cube, implying that the cubic seeds were mainly restricted to grow along the ⟨111⟩ directions. As the amount of $AgNO_3$ solution was increased to 3.5 mL (Figure 3f), cubes with obvious protuberant corners were observed, generating a morphology similar to that of an octapod. When the amount of $AgNO_3$ solution was increased to 6.5 mL (Figure 3g), larger octapods were obtained. A careful analysis indicates that the rudiment of high-index planes started to appear at each corner of the octapod. The octapods finally evolved into trisoctahedrons when the volume of $AgNO_3$ solution reached 10 mL (Figure 3h). When the amount of $AgNO_3$ solution was further increased to 14 mL, the recessed regions between adjacent trigonal pyramids were filled with Ag atoms to form nearly flat faces (Figure S6b). This transformation from a Ag cube to a Ag trisoctahedron is similar to what was observed for the Au trisoctahedron, during which the eight corners of a cube were pulled out and sharpened at the tips.[7]

In order to elucidate the mechanism involved in the formation of Ag concave octahedrons, we conducted a set of experiments using the standard procedure, except for the use of different concentrations for AA. It is not unreasonable to expect that increasing the concentration of AA (reductant) will increase the reduction rate for $AgNO_3$ and thus the deposition rate for Ag atoms. As shown in Figure S7, concave octahedrons were only formed at relatively high concentrations of AA. In contrast, octahedrons with flat faces were obtained when the concentration of AA was lowered relative to that used in the standard procedure. These observations indicate that fast reduction of $AgNO_3$ would enlarge a Ag nanocube along the ⟨100⟩ directions by preferentially depositing Ag atoms onto the {100} side faces. Consequently, concave structures were produced on the newly formed {111} facets. It is worth pointing out that the growth of Ag cubic seeds was mainly confined to the ⟨100⟩ directions in this case, which could be attributed to the absence of a capping agent such as poly(vinyl pyrrolidone) (PVP) or Br^- that could selectively bind to the {100} facets and retard their growth.[8] Although the mechanism involved in the formation of Ag concave trisoctahedrons is yet to be resolved, it seems to be that the Cu^{2+} ions were responsible for promoting the growth of {111} facets or retarding the growth of {100} facets of a cubic seed. This proposed mechanism is supported by the fact that the addition of $CuCl_2$ or $CuSO_4$ instead of $Cu(NO_3)_2$ into the reaction solution gave products with similar morphologies (data not shown). The mechanism might be related to the concept of underpotential deposition reported by Mirkin and co-workers for manipulating the growth habit of Au nanostructures with Ag^+ ions.[9] In a sense, the role played by Cu^{2+} ions seems to be somewhat complementary to what was provided by PVP and citrate in generating Ag cubes and octahedrons, respectively.[10]

The concave morphology associated with the new Ag nanocrystals makes them interesting candidates for investigating the shape dependence of SPR and SERS properties. Figure S8 gives UV-vis spectra taken from aqueous suspensions of the Ag nanocrystals depicted in Figure 3, clearly showing that the major SPR peak was continuously shifted from 425 to 545 and 530 nm, respectively, as the Ag cubic seeds evolved into concave octahedrons and trisoctahedrons. However, the number of resonance peaks was essentially unchanged because the symmetry was largely preserved during shape evolution.[11] In another study, 75 nm Ag concave octahedrons, Ag concave trisoctahedrons, and Ag octahedrons with flat faces (i.e., conventional octahedrons) were compared in terms of SPR and SERS properties. Figure 4a shows UV-vis spectra taken from aqueous suspensions of these nanocrystals. While the positions of their major

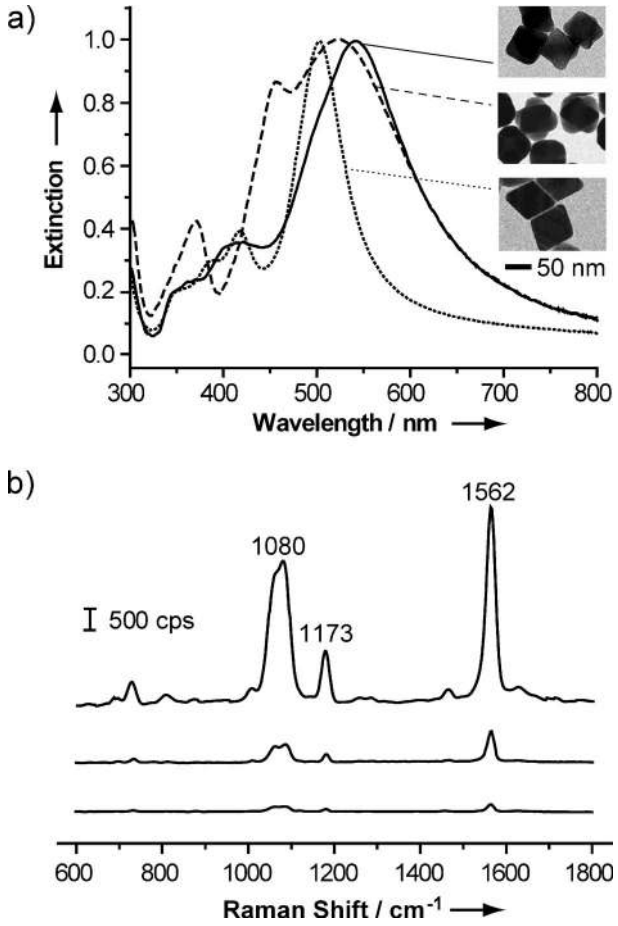

Figure 4. a) UV/Vis spectra of aqueous suspensions of Ag nanocrystals of 75 nm in size but in different shapes: concave octahedrons (solid curve), concave trisoctahedrons (dash curve), and conventional octahedrons (dot curve). Insets are typical TEM images of the Ag nanocrystals. b) Solution-phase SERS spectra of 1,4-BDT adsorbed on the concave trisoctahedrons, concave octahedrons, and conventional octahedrons (from top to bottom). All samples were suspended in water and the suspensions had the same particle concentrations. The SERS spectra were recorded with $\lambda_{ex} = 514$ nm, $P_{laser} = 2$ mW, and $t = 30$ s.

SPR peaks were located in the same region, the concave octahedrons and trisoctahedrons showed relatively broader peaks relative to that of conventional octahedrons. Unlike the conventional octahedrons, the peak at ca. 420 nm disappeared for the concave octahedrons. In addition, a distinct peak at ca. 365 nm and a shoulder peak at ca. 450 nm next to the major peak were observed for the concave trisoctahedrons. Figure 4b compares the SERS spectra of 1,4-benzenedithiol (1,4-BDT) adsorbed on the surfaces of these three different nanocrystals. The spectra were recorded from aqueous suspensions with roughly the same particle concentration. Based on the phenyl ring stretching mode at 1562 cm^{-1},[12] the SERS enhancement factors (EFs) were estimated as 5.7×10^5, 1.8×10^5, and 4.6×10^4 (see Supporting Information for detailed calculation) for the concave trisoctahedrons, concave octahedrons, and octahedrons, respectively. If we take into account their difference in intraparticle gaps, tips, and edges where SERS hot spots tend to be located,[13] it will not be difficult to understand the observed difference in EF. The Ag concave trisoctahedron contains many intraparticle gaps, tips, and edges, and thus is supposed to be rich of hot spots, should give the strongest SERS signals. Hot spots can also be created in the curved cavities of a concave octahedron, leading to a higher EF than the conventional octahedron with flat side faces. Since the three types of Ag nanocrystals had a similar major SPR peak, the possibility of wavelength-dependent enhancement,[14] where the SERS activity would be maximized when the excitation source matched the SPR peak of the nanocrystals, could be ruled out.

In summary, we have demonstrated, for the first time, a facile approach to the synthesis of Ag nanocrystals with concave surfaces by controlling the growth habit of Ag cubic seeds in an aqueous solution. Specifically, four types of concave nanocrystals, including octahedron, cube, octapod, and trisoctahedron, were obtained by controlling the growth of a Ag nanocube along either ⟨100⟩ or ⟨111⟩ directions. The as-prepared concave octahedrons and trisoctahedrons gave SERS signals approximately 4 and 12 times stronger, respectively, than the conventional octahedrons with a similar size. These concave nanocrystals represent an important addition to the vast varieties of convex Ag nanocrystals that have been prepared using chemical methods. Considering their distinct SPR and SERS properties, it is expected that these concave nanocrystals made of Ag may find widespread use as SRES substrates for both analytical and biomedical applications, as well as in catalysis.

Received: July 25, 2011
Published online: September 12, 2011

Keywords: concave nanoparticles · seeded growth · silver · surface-enhanced Raman scattering

[1] a) J. He, I. Ichinose, T. Kunitake, A. Nakao, Y. Shiraishi, N. Toshima, *J. Am. Chem. Soc.* **2003**, *125*, 11034; b) H. I. Peng, C. M. Strohsahl, K. E. Leach, T. D. Krauss, B. L. Miller, *ACS Nano* **2009**, *3*, 2265; c) Y. Wu, Y. Li, B. S. Ong, *J. Am. Chem. Soc.* **2007**, *129*, 1862.

[2] a) N. R. Jana, L. Gearheart, C. J. Murphy, *Chem. Commun.* **2001**, 617; b) Y. Sun, Y. Xia, *Science* **2002**, *298*, 2176; c) P. Brendan, K. Vladimir, *Chem. Mater.* **2008**, *20*, 5186; d) R. Jin, Y. Cao, C. A. Mirkin, K. L. Kelly, G. C. Schatz, J. G. Zheng, *Science* **2001**, *294*, 1901; e) J. Zhang, S. Li, J. Wu, G. C. Schatz, C. A. Mirkin, *Angew. Chem.* **2009**, *121*, 7927; *Angew. Chem. Int. Ed.* **2009**, *48*, 7787.

[3] a) X. Huang, S. Tang, H. Zhang, Z. Zhou, N. Zheng, *J. Am. Chem. Soc.* **2009**, *131*, 13916; b) J. Zhang, M. R. Langille, M. L. Personick, K. Zhang, S. Li, C. A. Mirkin, *J. Am. Chem. Soc.* **2010**, *132*, 14012.

[4] a) N. Tian, Z. Zhou, S. Sun, Y. Ding, Z. Wang, *Science* **2007**, *316*, 732; b) H. Zhang, W. Li, M. Jin, J. Zeng, T. Yu, D. Yang, Y. Xia, *Nano Lett.* **2011**, *11*, 898; c) C. L. Lu, K. S. Prasad, H. L. Wu, J. A. Ho, M. H. Huang, *J. Am. Chem. Soc.* **2010**, *132*, 14546.

[5] Y. Ma, Q. Kuang, Z. Jiang, Z. Xie, R. Huang, L. Zheng, *Angew. Chem.* **2008**, *120*, 9033; *Angew. Chem. Int. Ed.* **2008**, *47*, 8901.

[6] a) Ref. [4a]; b) N. Tian, Z. Zhou, S. Sun, *J. Phys. Chem. C* **2008**, *112*, 19801.

[7] H. L. Wu, C. H. Kuo, M. H. Huang, *Langmuir* **2010**, *26*, 12307.

[8] a) B. J. Wiley, Y. Chen, J. M. McLellan, Y. Xiong, Z. Y. Li, D. Ginger, Y. Xia, *Nano Lett.* **2007**, *7*, 1032; b) Z. Zhang, B. Zhao, L. Hu, *J. Solid State Chem.* **1996**, *121*, 105.
[9] M. L. Personick, M. R. Langille, J. Zhang, C. A. Mirkin, *Nano Lett.* **2011**, DOI: 10.1021/nl201796s.
[10] J. Zeng, Y. Zheng, M. Rycenga, J. Tao, Z. Y. Li, Q. Zhang, Y. Zhu, Y. Xia, *J. Am. Chem. Soc.* **2010**, *132*, 8552.
[11] A. Tao, P. Sinsermsuksakul, P. Yang, *Angew. Chem.* **2006**, *118*, 4713; *Angew. Chem. Int. Ed.* **2006**, *45*, 4597.
[12] a) M. Osawa, N. Matsuda, K. Yoshii, I. Uchida, *J. Phys. Chem.* **1994**, *98*, 12702; b) J. Y. Gui, D. A. Stern, D. G. Frank, F. Lu, D. C. Zapien, A. T. Hubbard, *Langmuir* **1991**, *7*, 955.
[13] M. J. Mulvihill, X. Y. Ling, J. Henzie, P. Yang, *J. Am. Chem. Soc.* **2010**, *132*, 268.
[14] A. D. McFarland, M. A. Young, J. A. Dieringer, R. P. Van Duyne, *J. Phys. Chem. B* **2005**, *109*, 11279.

